Decoding the interference signal in white light interferometry for precision temperature sensing

Author: Jordi Piñol Febrero
IEEC, Carrer de Can Magrans, s/n, 08193 Cerdanyola del Vallès, Spain.
Faculty of physics, University of Barcelona, Diagonal 645, 08028 Barcelona, Spain.

Advisors: David Roma Dollasse, Miquel Nofrarias Serra

Abstract: Thermal fluctuations have a key role in the performance of LISA space mission, which aims to detect gravitational waves. Equipment based on White Light Interferometry (WLI) is a promising technology to measure microkelvin thermal fluctuations at very low frequencies. The aim of this project, carried out by IEEC researchers, is to achieve measuring temperature fluctuations as low as 1 $\mu K/\sqrt{Hz}$ in the 1 Hz down to 0.1 mHz range. The interference output signal obtained by the photodiode utilized in IEEC installations is described using a physical model, where the measured intensity is deduced from the interaction of electromagnetic waves within the equipment. Expressions for the outputs of the sensing and reference interferometers are provided, allowing for the absolute temperature measurement through the utilization of the cross-correlation function between the reference and sensing signals. It is shown that the adjustment of the coherence length of the incident white light facilitates the measurement process by reducing sensitivity to noise.

I. INTRODUCTION

For the last few decades, considerable interest has been expressed in measuring gravitational waves since the aforesaid do not interact with matter in the way electromagnetic waves do. The information that they carry about their sources is more far-reaching than the one carried by the electromagnetic waves [1].

Gravitational waves were predicted by Einstein in 1916 one year after his theory of Relativity, and were observed for the first time in 2015 [2]. The frequency of these gravitational waves gives information about the mass of the source. The frequencies regarding these events are typically in a range between 10^4 and 10^{-18} Hz [1].

On-ground interferometers, measuring from the surface of Earth, are not capable of measuring gravitational waves with frequencies under 1 Hz, due to fluctuating gravitational gradients and seismic noise on Earth [3].

A space-based gravitational wave observatory, the LISA (Laser Interferometer Space Antenna) mission, is being carried out at present with the aim to be launched in the 2030s. The project is led by the European Space Agency (ESA). LISA mission is based on laser interferometry between free-flying test masses inside a drag-free spacecraft orbiting the Sun at 1 AU, about 20 degrees behind the Earth in its orbit. The observatory will be based on three arms with six active laser links, between three identical spacecraft in a triangular formation separated by 2.5 million km. Laser interferometers will measure the pm pathlength variations caused by gravitational waves [4].

Precise control over thermal fluctuations is paramount for the successful operation of gravitational wave detectors, including the LISA mission. Unregulated thermal disturbances can introduce perturbations that compromise detector performance, resulting in measurement errors and reduced sensitivity in accurately detecting gravitational waves. By implementing effective thermal management strategies, these fluctuations can be characterized, ensuring a stable and controlled environment conducive to precise gravitational wave measurements.

Temperature measurement and control are ubiquitous but generally routine aspects of many precision experiments. When a high degree of control is needed common practice is to use a multi-layer thermal enclosure and high sensitivity thermistors as the control sensors. Due to their inherent Johnson noise these sensors typically demonstrate a temperature resolution of a few μK at 1 s integration time [5]. This can be improved by increasing the power to the device, but soon self-heating becomes a limiting factor. The best reported resolution with thermistors we are aware of is ~ $20\mu K/\sqrt{Hz}$ at 0.1 mHz [6]. In environments like those found in a gravitational wave detector, where measurements with traditional electrical temperature sensors might not be effective, optical fiber sensors are a good alternative.

Optical fibers have garnered significant attention in various sensor fields due to their properties, including multiplexing capability, high flexibility, low propagation loss, high sensitivity, cost-effectiveness, compact size, accuracy and simultaneous sensing capability. Additionally, optical fibers possess the advantageous feature of being poor thermal and electrical conductors, which further enhances their suitability for our specific applications. [7].

In this project, carried out by IEEC researchers in collaboration with INESCTEC, it is being developed an absolute temperature measurement equipment based on WLI

Electronic address: pinyol@ieec.cat

[8]. The scheme that is being implemented is depicted in Figure 1. The main optical system consists in two parts, namely, the interrogation system and the sensing head block. The interrogation system is based on a Mach-Zehnder interferometer (MZI) couplet to a piezoelectric transducer (PZT) in one of the arms to modulate the optical path. The sensing head block is composed by two groups of distinct Fabry-Perot interferometers (FPIs): one is used as sensor and the other as reference.

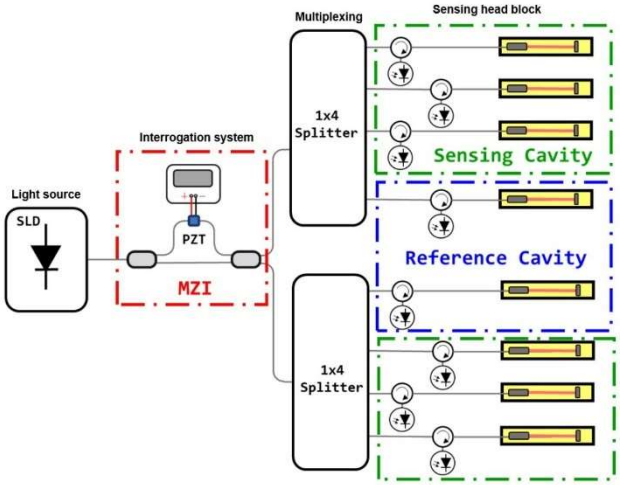

Figure 1. Scheme that is being implemented.

II. PRINCIPLE OF ABSOLUTE TEMPERATURE MESUREMENT

The IEEC equipment operates on the fundamental principle of measuring the peak signal generated by the combination of light beams within two interferometers. In the presence of an unknown temperature, the sensing Fabry-Perot Interferometer (FPI) with a high coefficient of thermal expansion (CTE), demonstrates an Optical Path Difference (OPD) specific to that temperature. By modulating the OPD of the interrogator through voltage application to the Piezoelectric Transducer (PZT), maximum interference occurs when both OPDs are equal. Measuring that maximum interference would lead us to know the OPD, and with that we can obtain the temperature.

Due to the practical limitations of directly measuring the size of the interrogator interferometer with sufficient accuracy, the utilization of a reference interferometer becomes necessary. The reference interferometer is housed within a sleeve composed of a material with a low CTE. It serves as a reference against which we compare the time delay between its own signal maximum and the maximum of the sensor interferometer. This time delay is measurable and exhibits a linear relationship with respect to the corresponding temperature. By leveraging this correlation, we can accurately determine the temperature.

While the experimental information is primarily extracted from the output signal of the photodiode, the development of a comprehensive physical model is essential to support and enhance the understanding of the obtained results. Predicting the signal through a mathematical model serves as a valuable tool for comprehending why the signal exhibits specific characteristics and behaviours, and how these align with the underlying theoretical framework.

I. ANALYSIS OF THE SIGNAL AT THE PHOTO-DETECTOR

In order to derive a mathematical expression that accurately describes the intensity of the photodiode, it is imperative to analyse the various components of the electromagnetic field throughout the experimental setup (Figure 1). By studying these components meticulously, we can establish a refined mathematical model that better aligns with the observed data in the laboratory.

Each time the light wave $\mathrm{E(t)} = \exp(-\mathrm{iwt})$ propagates through a distinct optical path, a phase term is incorporated into the wave equation that characterizes the light. As a result, in the proximity of the photodiode, the electromagnetic field can be described by the following expression:

$$E_T = E(t + \tau_P) + T \cdot E(t + \tau_F) \tag{1}$$

Where $\tau_P = \Delta L_P / c$ with c being the speed of light, is the time associated with the displacement of the OPD produced by the PZT, τ_F is the time associated with the displacement produced by the FPI, which is ultimately associated with the temperature, and T is the transmission coefficient associated to the FPI. As all the relevant information referred to the temperature is carried in the phase of the electromagnetic wave, T will be considered 1 to simplify the mathematical deduction.

The intensity of the light at this point, which corresponds to the signal received by the photodiode, can be expressed in terms E_T as follows:

$$I_T = \langle |E_T|^2 \rangle = \langle |E_T \cdot {E_T}^*| \rangle \tag{2}$$

Where ${E_T}^*$ is the conjugate of E_T. Therefore, when calculating I_T we obtain a combination of the terms in E_T multiplied by their conjugates, resulting in:

$$\begin{aligned} I_T &= \langle |E(t+\tau_P) \cdot E(t+\tau_P)^*| \rangle + \\ &= +\langle |E(t+\tau_F) \cdot E(t+\tau_F)^*| \rangle + \\ &= +\langle |E(t+\tau_F) \cdot E(t+\tau_P)^*| \rangle + \\ &= +\langle |E(t+\tau_P) \cdot E(t+\tau_F)^*| \rangle \end{aligned} \tag{3}$$

The first two terms in the expression are considered constants, and their sum is conveniently normalized to 1 for simplicity. The last two terms, which are modulated in time, encompass the relevant information related to the temperature measurement. To further analyse and extract the desired information, we can apply a mathematical relationship to equation (4), as it is done in [10].

$$I_T = 1 + 2 \cdot Re\{\langle E^*(t+\tau_F) \cdot E(t+\tau_P)\rangle\} \quad (4)$$

We can rewrite the electromagnetic wave associated with I_T as follows:

$$\begin{aligned}\langle E^*(t+\tau_F) \cdot E(t+\tau_P)\rangle &= \langle e^{iw(t+\tau_F)} \cdot e^{-iw(t+\tau_P)}\rangle \\ &= \langle e^{iw(t)} \cdot e^{-iw(t+\tau_P-\tau_F)}\rangle \\ &= \langle E^*(t) \cdot E(t+\tau_P-\tau_F)\rangle\end{aligned} \quad (5)$$

It can be noticed that this term that describes I_T corresponds to the autocorrelation function of $E(t)$, as it is the correlation $R_E(\Delta\tau)$ of the electromagnetic signal with a delayed copy of itself as a function of the delay $\Delta\tau = \tau_P - \tau_F$. We can now express (5) in terms of the autocorrelation:

$$I_T(\Delta\tau) = 1 + 2 \cdot Re\{R_E(\Delta\tau)\} \quad (6)$$

From the Wiener–Khinchin theorem, we know that the autocorrelation function of a wide-sense-stationary random process has a spectral decomposition given by the Fourier transform of the power spectral density function (PSDF) of that process. Initially the PSDF was assumed to have a step function form in [9]. However, it is reasonable to consider a Gaussian distribution for the PSDF of the incident light [10-14]. In fact, upon examining the specification sheet provided by the light manufacturer [15], it is apparent that the light possesses a Gaussian form characterized by specific values of central wavelength and bandwidth. Therefore, the PSDF equation that accurately describes the manufacturer's specifications is given by:

$$S(v) = \frac{1}{\sqrt{\pi}\Delta v} exp\left[-\left(\frac{v - v_0}{\Delta v}\right)^2\right] \quad (7)$$

Where v_0 is the mean frequency, and Δv is the bandwidth of the source. The autocorrelation function can be expressed in terms of $S(v)$, and terms of $\Delta\tau$:

$$R_E(\Delta\tau) = \int_{-\infty}^{\infty} S(v) exp(-i2\pi v\Delta\tau) dv \quad (8)$$

If we solve the complex integration, and substitute it into (6), we obtain:

$$I_T(\Delta\tau) = 1 + e^{-(\pi\Delta v\Delta\tau)^2} \cdot \cos(2\pi v_0\Delta\tau) \quad (9)$$

$I(\Delta\tau)$ is commonly expressed in terms of the OPD length. If we change the domain of time to the domain of space using $\Delta\tau = \Delta L_{P-F}/c$, and introducing the concept of coherent length $\sigma = c/\Delta v$, we can give the sensing and the reference interferometer outputs by:

$$I_s(\Delta L_S) = 1 + e^{-\left(\frac{\pi}{\sigma}\Delta L_S\right)^2} \cdot \cos\left(\frac{2\pi}{\lambda_0}\Delta L_S\right) \quad (10)$$

$$I_R(\Delta L_R) = 1 + e^{-\left(\frac{\pi}{\sigma}\Delta L_R\right)^2} \cdot \cos\left(\frac{2\pi}{\lambda_0}\Delta L_R\right) \quad (11)$$

These longitudes are given by the length difference between both interferometers' arms: $\Delta L_S = L_P - L_S$, and $\Delta L_R = L_P - L_R$. Those last values are given by:

$$L_P(t) = n_1\big(L_1 + e_V V(t)\big) \quad (12)$$

$$L_S(T) = n_2\big(L_2 + L_3(\alpha_T \Delta T)\big) \quad (13)$$

$$L_R = n_2(L_2 + L_4) \quad (14)$$

Where:

- n_1 and n_2 are the respective refraction index of each interferometer. Both values will be considered 1 as n_2 correspond to the refraction index of the vacuum, and n_1 the one of the air, which is a reasonable approximation.
- L_1 is the arm length difference of the interrogation interferometer.
- $e_V V(t)$ is the induced arm length associated to the PZT. e_V is the coefficient which translates the applied voltage to an effective displacement and $V(t)$ is the applied voltage.
- L_2 is twice the length of the cavity of the sensor.
- L_3 is twice the length of the metallic sleeve which size changes with temperature.
- L_4 is twice the length of the reference sleeve which size does not depend on temperature.
- $\alpha_T \Delta T$ is the size change of the metallic sleeve, where α_T is the CTE of the material of the sleeve and ΔT the temperature change.

So finally, assuming $L_1 = L_2$, and a linear voltage applied to the PZT, we get the intensity of the photodiode for our specific set-up as a function of time, which is ultimately, what we will be measuring in the laboratory.

$$I_s(t) = \left[1 + e^{-\left(\frac{\pi}{\sigma}(e_v\beta t - S)\right)^2} \cdot \cos\left(\frac{2\pi}{\lambda_0}(e_v\beta t - L_S)\right)\right] \quad (15)$$

$$I_R(t) = \left[1 + e^{-\left(\frac{\pi}{\sigma}(e_v\beta t - L_R)\right)^2} \cdot \cos\left(\frac{2\pi}{\lambda_0}(e_v\beta t - L_R)\right)\right] \quad (16)$$

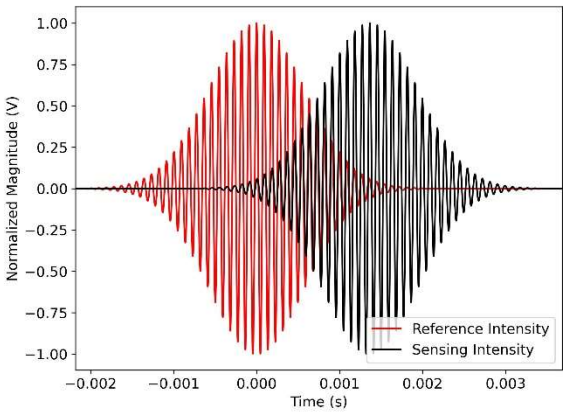

Figure 2. Comparison between sensing and reference intensities.

As we will be measuring the time difference between the two maximums, we can define the origin of time in the maximum of the reference intensity.

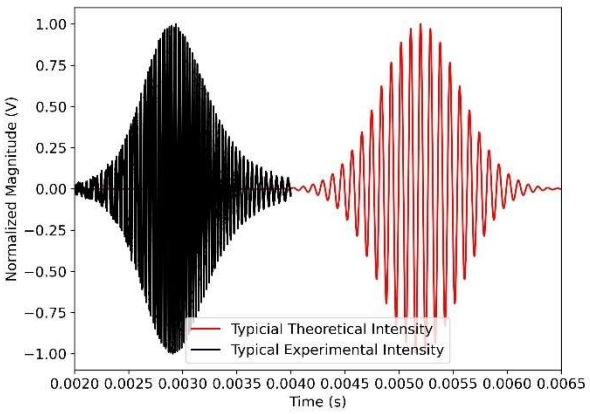

Figure 3. Comparison between the theoretical intensity deduced in Eq. 15 and a typical experimental intensity.

The consistency of our results can be assumed based on the congruence with findings reported by other researchers investigating similar white light interferometers. Several studies [11-14] have reported identical results, which reinforces the validity and reliability of our findings. Additionally, Figure 3 highlights the similarities between the experimental and theoretical intensities, providing further evidence of the agreement between our experimental data and the theoretical predictions.

III. TEMPERATURE ACQUISITION

After obtaining the signals for the reference and sensor interferometer, the next step is to compute the cross-correlation function between them. The resulting cross-correlation function is depicted in Figure 4.

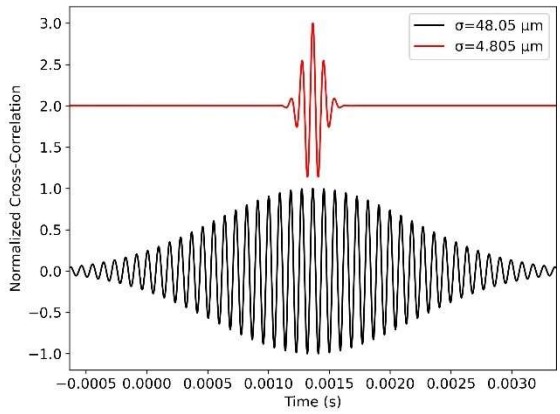

Figure 4. Cross-correlation function for different values of σ, with the offset between the two signals added solely for visual purposes.

The maximum value of the cross-correlation function can be interpreted as the time displacement (Δt) required between the two signals to achieve the highest degree of similarity or alignment between them. The increment of temperature of the sensing FPI respect to the reference FPI can now be determined based on this Δt and it can be expressed as follows:

$$\Delta T = \frac{e_V \beta}{L_3 \alpha_T} \Delta t \tag{17}$$

We have been able to establish a quantitative relationship for the absolute temperature measurement.

IV. CONCLUSIONS

A white light source is directed into a Mach-Zehnder interferometer (MZI). The output from the MZI is then coupled into the Fabry-Perot interferometer (FPI) cavities. Within each FPI cavity, an optical output signal is generated, which is subsequently converted into an electrical current using a photodiode. The resulting electrical signals are sampled and processed to extract precise temperature data.

This measurement approach involves the use of both a sensor cavity and a reference cavity per sensing channel, enabling differential temperature measurements. By combining the obtained differential measurement with the pre-calibrated and fixed temperature set-point of the reference cavity, an absolute temperature measurement can be achieved.

By establishing mathematical expressions for both the signal and reference interferometers (Equations 15-16), we can determine the time shift between them through the cross-correlation function (Figure 7). This time shift allows us to calculate the temperature using Equation 17. Through this investigation, we have gained valuable insights into the factors that shape the temperature measurement process.

To enhance the quality of temperature measurements, we can increase the product of L_3 and α_T in Equation 17. However, it is important to note that increasing the value of L_3 would result in a larger equipment size. Hence, it has been set a limit of 80 mm for L_3 to strike a balance between measurement quality and practical considerations. Additionally, the highest value of α_T available for our measurements is already being used.

The modification of the coherent length does not alter the measured temperature, as demonstrated in Figure 7, where both autocorrelations exhibit their maximum at the exact same value of Δt. Instead, the purpose of modifying the coherent length is to enhance the measurement process itself. In Fig. 7 (with $\sigma = 48.05\ \mu m$), when introducing noise to the intensities, there is a possibility that the highest peak may not correspond to the actual desired peak. This can occur when consecutive peaks have similar values, and noise causes a secondary peak to appear higher than the expected one. By utilizing a source with a smaller coherent length, such as $\sigma =$

4.805 μm (bigger bandwidth), we can observe from Figure 7 that the autocorrelation becomes less sensitive to noise. We can deduce that the difference between two consecutive maximums in the autocorrelation function are inversely proportional to the coherence length, lowering this value minimizes the possibilities of measuring a secondary peak as the peak of interest.

Despite the consistency of the results obtained for the intensities with the existing literature [10-14], we have encountered certain discrepancies when comparing them with the laboratory data. It is important to note that all the mathematical deductions were based on the assumption of a linear behaviour of the PZT. However, the linearity of the PZT has been called into question by the researchers at IEEC. As of today, ongoing studies at the institute are exploring alternative behaviours of the PZT, which may provide insights into the observed discrepancies.

Acknowledgments

I would like to express my gratitude to all the members of the IEEC team for giving me the opportunity to be a part of this project. Furthermore, I wish to extend my special thanks to my advisors, David Roma and Miquel Nofrarias, for their guidance and support during the development of this work.

[1] Thorne, K. S. (1995). Gravitational Waves. arXiv:grqc/9506086

[2] B. P. Abbott et al. (LIGO Scientific Collaboration and Virgo Collaboration) Observation of Gravitational Waves from a Binary Black Hole Merger. Phys. Rev. Lett. 116, 061102 (2016)

[3] Pitkin, M. et al (2011). Gravitational Wave Detection by Interferometry (Ground and Space).

[4] Danzmann, K. et al (2017). LISA Laser Interferometer Space Antenna. A proposal in response to the ESA call for L3 mission concepts. https://arxiv.org/abs/1702.00786

[5] L. D. Bowers and P. W. Carr, “Noise measurement and the temperature resolution of negative temperature coefficient thermistors,” Thermochim. Acta 10, 129–142 (1974).

[6] Roma-Dollase, D.; Gualani, V.; Gohlke, M.; Abich, K.; Morales, J.; Gonzalvez, A.; Martín, V.; Ramos-Castro, J.; Sanjuan, J.; Nofrarias, M. Resistive-Based Micro-Kelvin Temperature Resolution for Ultra-Stable Space Experiments. Sensors 2023, 23, 145. https://doi.org/10.3390/s23010145

[7] Lee, B.H.; Kim, Y.H.; Park, K.S.; Eom, J.B.; Kim, M.J.; Rho, B.S.; Choi, H.Y. Interferometric Fiber Optic Sensors. Sensors 2012, 12, 2467-2486.

[8] Canizares P. et al., The diagnostics subsystem on board LISA Pathfinder and LISA

[9] Sensor read-out preliminary design. Doc. Ref.: LIRA-IEEC-WP240-RP-001 Issue: 1.0 Date: 21/02/22

[10] New signal processing algorithm for white light interferometry. Kim, Jeong Gon. Texas A&M University. 9800760.

[11] S. Chen, A. W. Palmer, K. T. V. Grattan, and B. T. Meggitt, "Digital signal-processing techniques for electronically scanned optical-fiber white-light interferometry," Appl. Opt. 31, 6003-6010 (1992)

[12] Kim, J.H. An All Fiber White Light Interferometric Absolute Temperature Measurement System. Sensors 2008. .8, 6825-6845.

[13] Kim JG. Absolute Temperature Measurement using White Light Interferometry. Curr. Opt. Photon. 2000;4:89-93.

[14] Kim, J.H. High Precision Signal Processing Algorithm for White Light Interferometry. Sensors 2008, 8, 7609-7635.

[15] Thorlabs Spec Sheet SLD1550P-A2 2.5 mW SLD, CWL=1550 nm, 90 nm 3 dB BW, Butterfly Package, PM Fiber, FC/APC